The International Journal of Advanced Manufacturing Technology (2018) 97:3925–3935
https://doi.org/10.1007/s00170-018-2236-y

ORIGINAL ARTICLE

Improved child-resistant system for better side impact protection

Lukasz Mazurkiewicz[1] · Pawel Baranowski[1] · Hamid Reza Karimi[2] · Krzysztof Damaziak[1] · Jerzy Malachowski[1] · Artur Muszynski[3] · Andrzej Muszynski[4] · Kjell Gunnar Robbersmyr[5] · Dario Vangi[6]

Received: 5 April 2017 / Accepted: 27 May 2018 / Published online: 4 June 2018

Abstract

The article presents a new solution of child-resistant systems to improve the safety of children transported in motor vehicles subjected to a side impact during a vehicle crash. The proposed concept works by means of implementation of an energy dissipation mechanism acting between a child restraint system anchorage and a restraint system seat. The effectiveness of the proposed system is evaluated using numerical analyses of a simplified basic model as well as more complex mechanical design of the mechanism. The latter is analyzed as a part of the child restraint system (CRS) together with a deformable model of an anthropomorphic test device of Q3 series. Tests outcomes clearly show a positive effect of application of the proposed energy dissipation system resulting in reduction of head and thorax acceleration and influencing a lower factor (index) of the head injury criteria. The presented solution shows that there is still a room for improvement of young passengers safety.

Keywords Crashworthiness · Crash simulation · Child-resistant systems · Finite element analysis · Side impact

1 Introduction

In 2005, costs associated with motor vehicle-related fatal and non-fatal injuries among 0–14-year-old children amounted to over 3.6 billion USD in the USA [1]. The statistics show that motor vehicle crashes are the leading cause of death among children both in the USA and Canada [2, 3]. The same fact applies to the European Region [4]. Despite a mandatory use of various child restraint systems (CRSs) and the existence of such regulations as UN/ECE Regulation 44, this situation has not changed over the last few years [5]. Researchers investigating the problem highlight the two most important issues that are still required to pay a special attention: constant misuse of a CRS [6–8] and the number of injuries due to a side impact, or near-side impact collision [9, 10].

Fortunately, there are some organizations involved in child safety which have undertaken the discussed problem. The most significant one is Australia's Child Restraint Evaluation Program (CREP) that started back at the end of the twentieth century. It proved that systematic research can reveal a vital set of guidelines for both rule makers and CRS makers [11]. Although the CREP program have been implemented for some time, the Australian experience and methodology have only recently received enough attention in the USA [12] with a provision proposed by the National Highway Traffic Safety Administration (NHTSA) [13].

In the European Union, recognition of the abovementioned problems led to preparation and implementation of a new standard: UN/ECE Regulation 129 [14]. According to the commission, one of the major improvements provided by this document (compared to the predecessor, Regulation 44) is better lateral impact protection achieved by means of a mandatory side impact test [15].

For example, many reports point to the seatbelts misuse as one of the important issues affecting safety [7, 16, 17]; however, presently, the only solution available on the market addressing this problem is the active tensioning system (ATS) introduced by Britax-Roemer. A side impact is also widely recognized as a very severe type of crash [15, 18, 19]. What

✉ Jerzy Malachowski
jerzy.malachowski@wat.edu.pl

[1] Department of Mechanics and Applied Computer Science, Faculty of Mechanical Engineering, Military University of Technology, Gen. S. Kaliskiego 2 str., Warsaw, Poland

[2] Department of Mechanical Engineering, Politecnico di Milano, via La Masa 1, 20156 Milan, Italy

[3] Idap Technology, Jagiellonska 55 str., Warsaw, Poland

[4] Automotive Industry Institute, Jagiellonska 55 str., Warsaw, Poland

[5] Department of Engineering Sciences, University of Agder, Gimlemoen 25A, Kristiansand, Norway

[6] University of Florence, Piazza San Marco 4, Florence, Italy

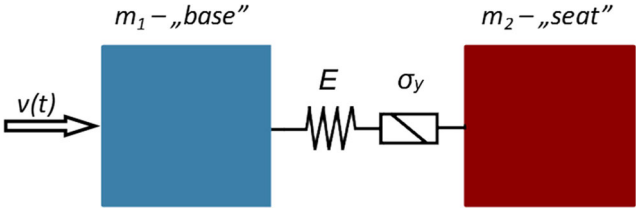

Fig. 1 Simple representation of CRS base and CRS seat

is alarming though is that so far the only “answer” for the new requirements given by CRS producers is to add a portion of energy absorbing foam (a form of additional structural solution) in the sideway zones of the CRS headrest, while the main concept of seat design remains still the same for years. Perhaps the best illustration of the situation in research on CRS design is the crash test conducted in 2009 in Sweden. It showed that Toyota Yaris, model year 2008 and Volvo 945, model year 1996, despite a 12-year difference, offer the same level of child protection, which is unacceptable in the case of adults (especially drivers) protection systems [20, 21].

The abovementioned crash test showed yet another issue related to the insufficient attention put on development of more safe CRS. It occurred that a normalized chest load of a child dummy seated in Toyota was two times higher compared to an adult driver dummy. Moreover, Kuppa et al. [18] showed the results of a crash test leading to similar conclusion.

In this paper, the authors present an innovative concept of a new, ISOFIX-mounted, CRS design. It is aimed at improving child protection during a lateral impact crash scenario by a proposition of a modification in the CRS design concept. A comparison of the basic (unmodified) CRS and the modified CRS concept are provided proving that the energy dissipation mechanism, with a principle of operation based on plastic deformation of a wire bent, reduces forces acting on a child body. In this study, finite element analyses (FEA), which have already proven their effectiveness in investigating many crash scenarios, were adopted [10, 22–24]. Only numerical studies of the CRS concept with dissipation system are presented without any validation data. This is due to the fact that the FE CRS model applied in the simulations was used to verify the proposed concept of the energy dissipation system. It is also the end-result of one of the stages during the realization of the project INNOTECH-K1/IN2/59/182901/NCBR/12 and other projects covering the CRS modeling and simulation. Based on the results obtained from projects, the prototype, which is much more complicated and has a completely different design, is being manufactured. Therefore, in this research, a validation of two different CRSs is missing the target.

2 The concept of the new energy dissipation system

The key concept of the currently produced CRS with ISOFIX anchorage is similar to the idea of non-stretching seatbelts. During an impact event, a child starts to decelerate together

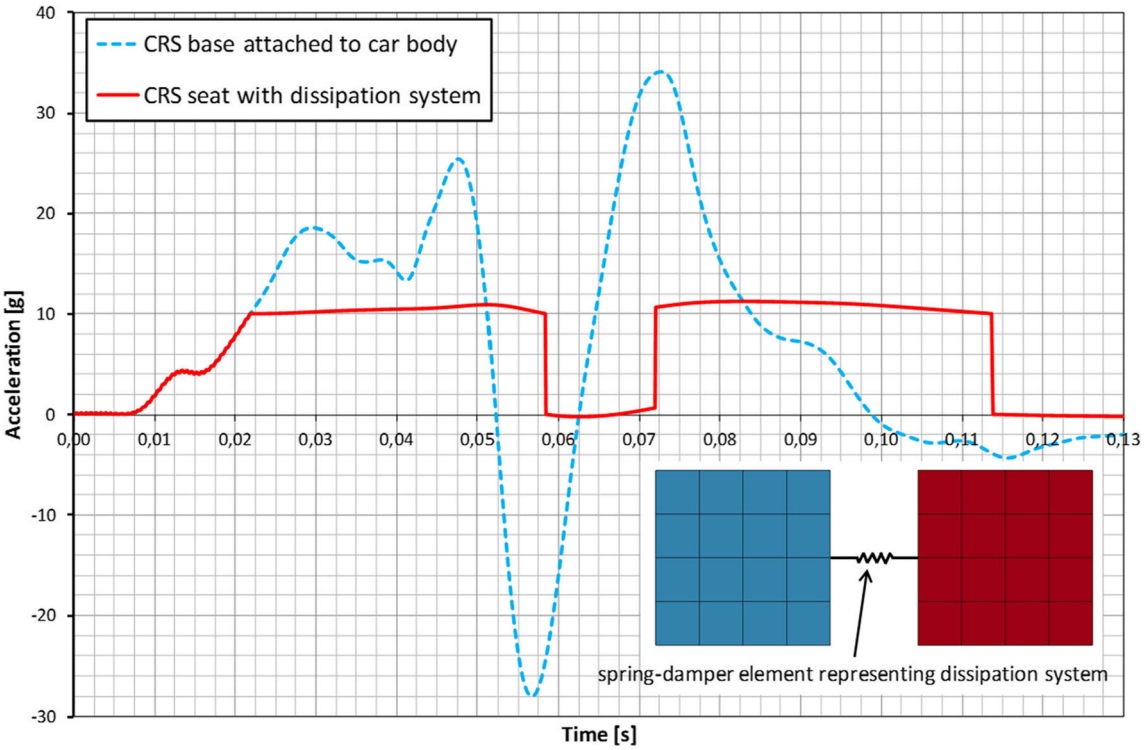

Fig. 2 Acceleration histories in the bodies representing CRS base and CRS seat

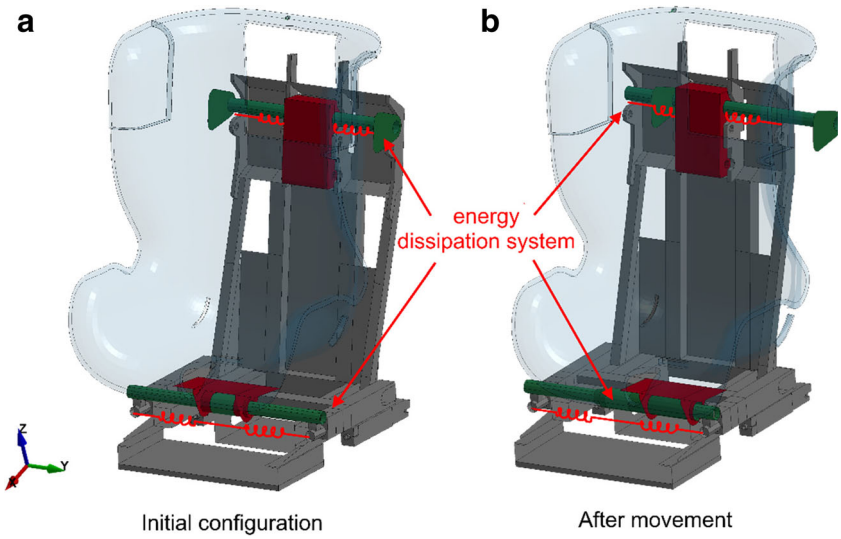

Fig. 3 CRS with energy dissipating elements

with a whole car body due to the fixed connection between the car and CRS during the impact. This enables to benefit from energy dissipation occurring in crumple zones and keeping the child away from a contact with inner parts of a car (at least in a frontal impact scenario). Staying with an adult seatbelts similitude, the new idea can be seen as introduction of their more sophisticated version.

Typical CRS for group 1 (the group designation according to old Regulation 44) consists of a base, which is connected to the car body via ISOFIX anchorage and a seat, mounted on the base, where a child actually sits. The most fundamental assumption behind the new concept is that during impact, CRS seat will be permitted to move independently to the base. Therefore, the seat with a child and the CRS base can be treated as separate bodies. This allows thinking about the CRS as multibody system consisted of two bodies connected each other with a kind of interface element—the concept has been already investigated in [25] and used to analyze vehicle crashes [26–28]. In the presented case, the elements that control the aforementioned relative movement of the base and the seat will be introduced. Figure 1 presents the simplest representation of such a system. It is assumed that the connector with inelastic properties placed between two bodies is used as an element responsible for energy dissipation.

The influence of the connector was investigated using a simple model shown in Fig. 1. The left body of the model, with prescribed mass $m_1 = 1000$ kg, represents the car body with base of the CRS connected to the car using ISOFIX. The right body, with prescribed mass $m_2 = 20$ kg, represents a seat of the CRS with a child sitting on it. The energy dissipation

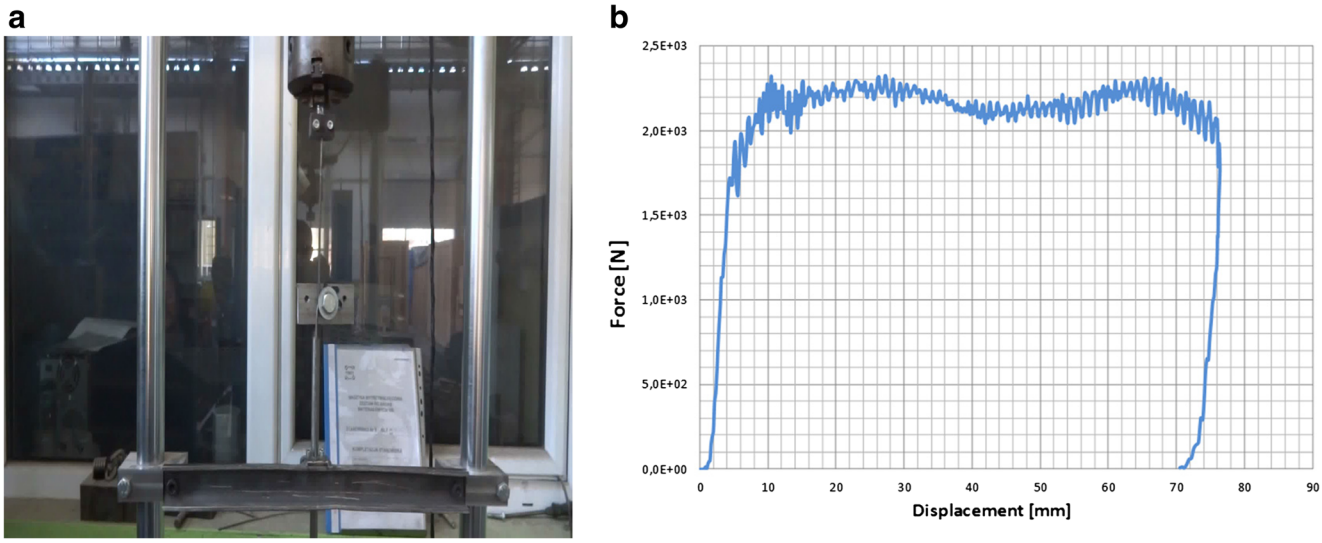

Fig. 4 **a** Test stand with a model of energy dissipation device and schematics of the device. **b** Typical force-displacement characteristic of energy dissipation device (the area under the curve represents the energy absorbed by the proposed mechanism in the test) (right)

Table 1 Material properties with associated parts of the CRS [38]

	Density ρ (kg/m^3)	Young modulus E (GPa)	Poisson ratio ν (−)	Yield stress Re (MPa)	Tangent modulus E_{tan} (MPa)
Steel	7850	210	0.3	400	1000
Polyamide	1130	3	0.3	85	100
Polypropylene (Tiplen)	900	1.3	0.45	7	(Table 2)
Headrest foam	60	0.00025	–	–	(Table 3)
Polystyrene foam	27	0.019	0.3	–	–

device was modeled using an inelastic spring element linking two bodies. The connector had an elastic—perfectly plastic characteristic—an equivalent of the Hookean substance connected in a series with the Saint-Venant's substance. In fact, this model represents a principle of operation of the proposed energy dissipation mechanisms.

The prescribed velocity in time $v(t)$ was applied to the body representing a base of CRS, as shown in Fig. 1. The velocity profile history was obtained using integration of an acceleration history taken from a side impact crash test of two cars.

Acceleration vs. time curves for the bodies representing "base" and "seat" are shown in Fig. 2. It can be seen that introduction of an inelastic connector drastically reduces maximum acceleration of the second body. It can be stated that, somehow, a filter was applied for the acceleration history of CRS attached to the car body.

3 Implementation of the energy dissipation solution into a real-world CRS

The basic principle of the dissipation systems is to transform kinetic energy into plastic deformation and fracture of a structure. Metallic thin-walled structures are one of the most widely used energy-absorbing elements due their excellent performance under axial loading, small initial impact force, or a long deformation process. Such structures have been extensively studied by many researches [29–31]. On the other hand, cellular elements with features such as outstanding properties in efficient energy absorption and excellent mechanical damping properties have been also investigated [32, 33]. Cutting damage of metal sheets, which shows that the work of friction forces and plastic deformation of the cut sheet can be used in a solution to dissipate energy, is also worth mentioning [34, 35].

All the above-mentioned solutions were analyzed in terms of possibilities for implementation in the CRS prototype. The modified CRS had to satisfy applicable standards. This meant that ISOFIX mount had to remain in place and CRS dimensions as well as total weight could not exceed certain values. Taken all above into consideration, it was decided to use a far more different solution: wire bent on a roll. In this case, the energy should be dissipated via plastic deformation of the introduced dissipation element and, to a lesser extent, via plastic deformation of CRS parts. The schematics of the final layout incorporating the new idea are shown in Fig. 3. As the basic model described above, in the new CRS design, two parts can be distinguished. The first part contains the

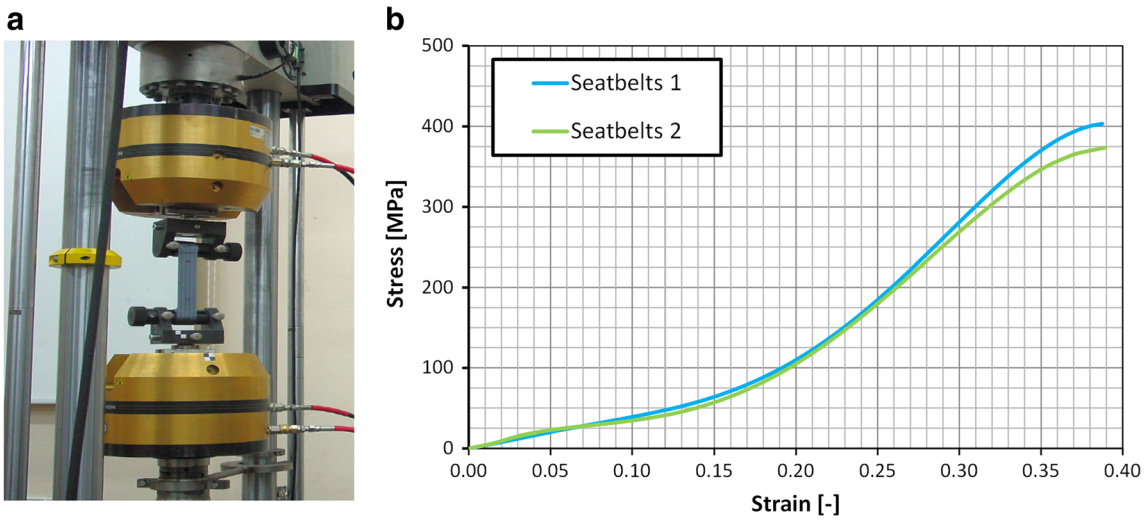

Fig. 5 **a** Test stand. **b** Stress-strain relationship for wide (1) and narrow (2) seatbelts

Table 2 Nonlinear characteristic of the plastic region of Tiplen (based on experimental data) [38]

Effective plastic strains	Effective stress (MPa)
0.00	7.0
0.019	17.0
0.045	20.5
0.070	22.0
0.150	23.5

ISOFIX anchorage and, thus, it is rigidly connected to the car body. The second part, where a child is actually seated, can move to the sides relative to the first one. The movement is controlled by elements responsible for energy dissipation.

The characteristic of a dissipation element was taken from experimental tests that were conducted at the Automotive Industry Institute (see Fig. 4). In the FE analyses, the dissipation elements were modeled using springs elements with a nonlinear force-displacement characteristic applied from the experiment performed.

4 Numerical simulation of improved CRS

The crashworthiness of a new design was virtually tested using the commercial code LS-Dyna [36]. The software is based on the finite element method (FEM) and uses an explicit scheme for time integration of a system of equations describing a motion. The FE model of the CRS consists of 146,599 elements and 118,974 nodes. Most of the structure was modeled using four-node shell elements utilizing Belytschko–Tsay formulation [37]. A typical approach and all the necessary steps required to develop a correct FE model of CRS can be found in Muszynski [38]. The aforementioned paper presents detailed information on a numerical FE model

Table 3 Nonlinear characteristic of the headrest foam (based on experimental data) [38]

Volumetric strains	Effective stress (kPa)
0.00	0
0.10	20
0.20	25
0.30	30
0.40	35
0.50	44
0.60	60
0.70	112
0.80	275
0.83	445

of a child seat and its validation based on the test results. An effect of modeling techniques and dynamic material behavior on the obtained results were also discussed. A methodology presented in the article was also used to develop FE model of the CRS with a new concept of a dissipation mechanism.

Proper representation of kinematics of the structure required definition of 24 contact pairs. In fact, obtainment of proper behavior of a contact algorithm was the most time-consuming part of the numerical model development. In all analyses, the interaction between all parts of the model was simulated using the contact procedure implementing the penalty method. The principal of this method can be described as placing normal interface springs between all nodes that belong to a penetrating surface ("slave surface") and their normal projections on the surface that is penetrated ("master surface") [36].

The material properties for steel, polyamide, polypropylene (tiplen), seatbelts, and foams were acquired experimentally and description of each test can be found in Baranowski et al. [23] and Muszynski [38]. Material characteristics and properties associated with different parts of the CRS are listed in Table 1.

During numerical modeling of a CRS, attention should be focused on the proper modeling of seatbelts. First, mechanical properties of the belt material were described based on the results obtained from uniaxial tension tests carried out for two different kinds of seatbelts [39]. Seatbelts stress-strain characteristics obtained from the experimental tests are presented in Fig. 5a. The data were entered into the selected constitutive model that provides a correct description of the belt material behavior during analyses. The numerical model of a harness system consisted of 2D elements, described using a fabric constitutive model, combined with 1D elements (seatbelt constitutive model). 2D seatbelt parts were finely meshed to accurately distribute contact forces between the dummy and the belt itself. Slipping of the belts in the buckle was simulated using a special feature available in LS-Dyna code called "slipring." No experimental data were available to match the friction parameters; therefore, a friction coefficient of 0.2 was used (based on the recommendations of James K. Day from Livermore Software Technology Corporation this value should usually be less than 0.3).

The CRS was enriched with a Q3 ATD. An FE model of a Q3 ATD represents a 3YO child weighting 14.5 kg. It consists of 165 different parts. Fully deformable ATD models developed by Humanetics Innovative Solutions are recognized as "standard" in crash test simulations. The company assures that all numerical ATD models reproduce behavior of the ATDs used in laboratory crash tests [39] (Tables 2 and 3).

A general concept of the analysis was to perform a crash test similar to the one described in UN/ECE Regulations 129, however, without side wall imitating interior of a car. The boundary conditions represent the situation when the child sits

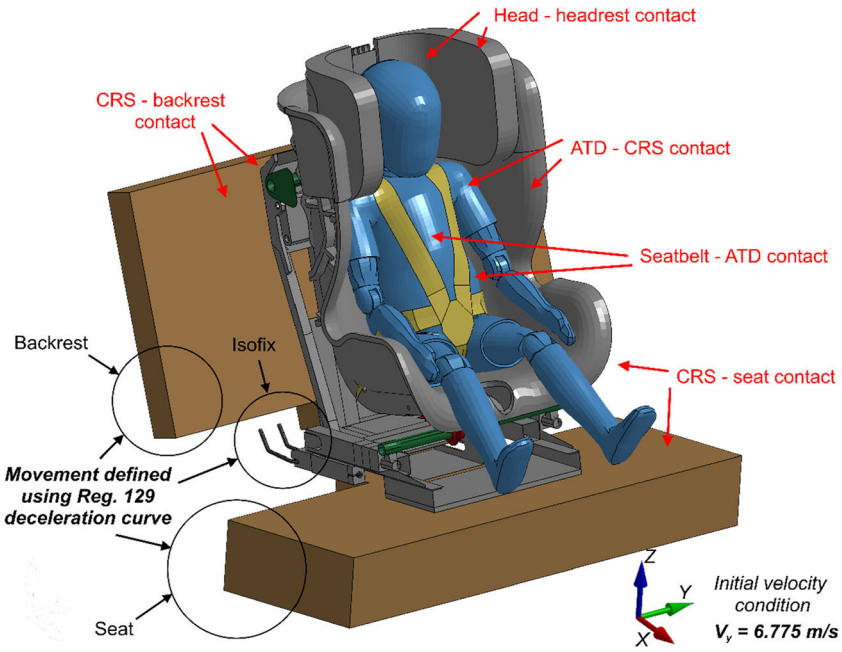

Fig. 6 FE model of CRS with child and applied boundary conditions

on the far side of the impact (during such a scenario the CRS with the child moves toward the center of a car). Therefore, no interaction with the vehicle body was assumed, and thus the door was not included in the model. The investigation was possible by applying the deceleration curve compliant with Regulation 129 to the seat, backseat, and ISOFIX mounts. Additionally, the initial velocity of the whole CRS-ATD FE model was defined as the maximum value of a curve (v = 6.775 m/s) according to the upper corridor curve defined in Regulation 129. Boundary conditions applied to the model are shown in Fig. 6.

Numerical simulations were performed for two versions of the CRS model. In the first one (test #1), the relative movement between the base and seat was blocked. This model can be assumed as a basic CRS, without any modifications. In the second model (test #2), the relative movement of the base and seat was allowed and energy dissipating elements were activated. The second model can be seen as a design reproducing the structural concept described in Section 2.

5 Results and discussion

In Fig. 7, qualitative analysis is presented with the selected stage of the CRS with ATD FE model movement for both cases. The relative movement of the seat vs. the CRS base can be clearly seen in the seat with the dissipation system. Also, noticeably smaller movement of the ATD's head can be noticed. The main assumption of dissipation system operation was that the energy should be dissipated via plastic

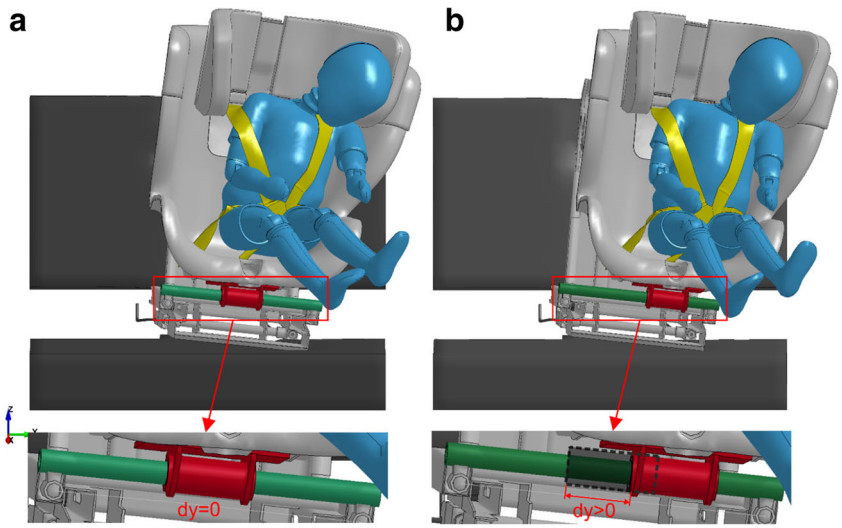

Fig. 7 **a** Basic—standard CRS case. **b** CRS with energy dissipation mechanism during side impact simulation. The movement of the seat relative to the base can be noticed in (**b**) picture

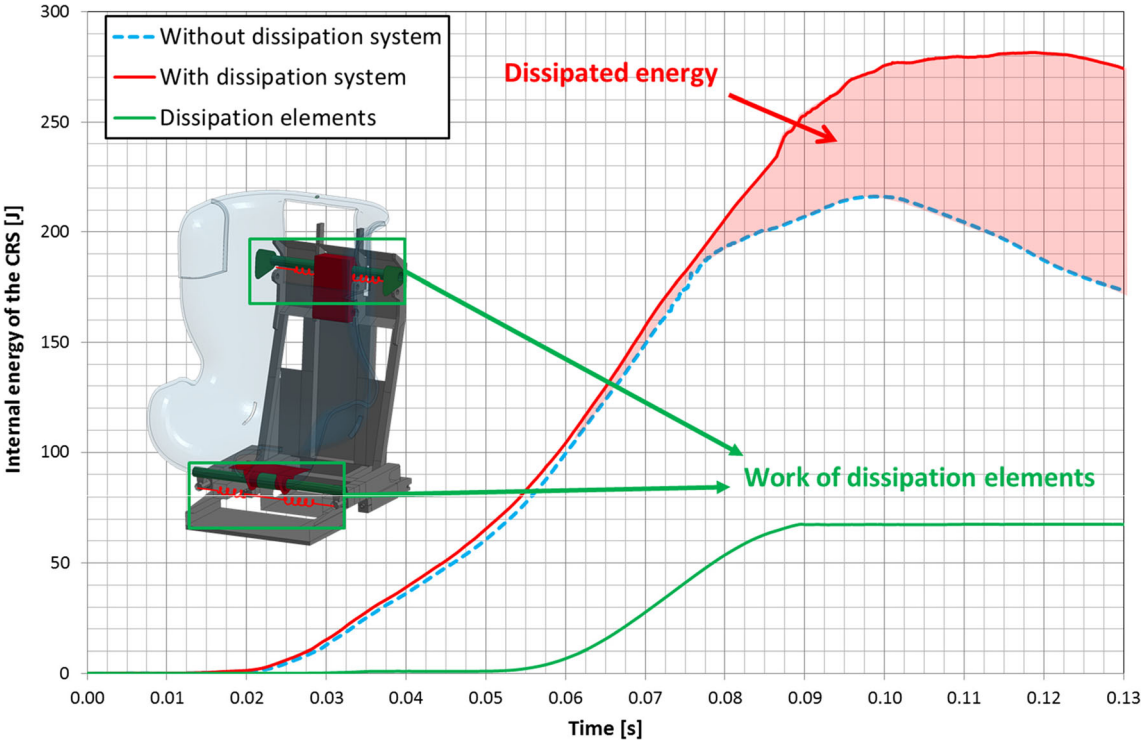

Fig. 8 Internal energy graph of the CRS elements for both tests with the work of dissipation elements included

deformation of the introduced dissipation element and to a lesser extent via plastic deformation of CRS parts. This is clearly confirmed in Fig. 8 showing an internal energy history of the CRS parts, including the work of dissipation elements representing the steel wire. In test #1, a smaller amount of energy was consumed by the CRS parts (max: 216 J), than

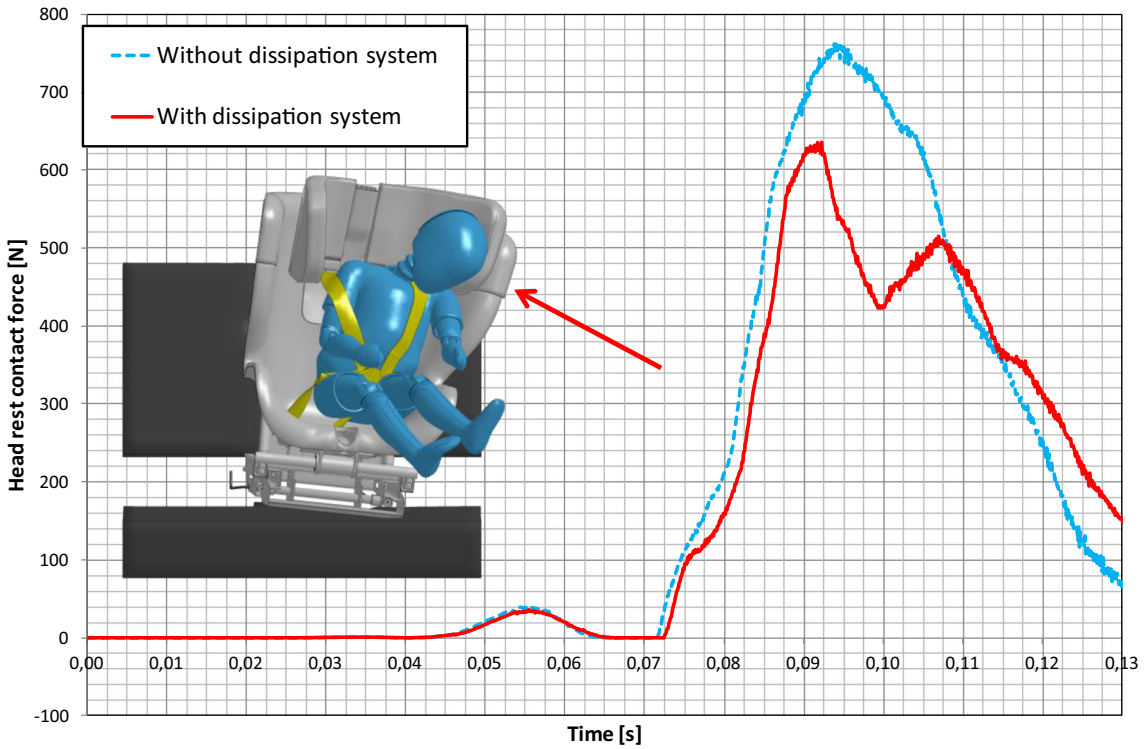

Fig. 9 Contact force between the ATD head and the CRS headrest in both tests

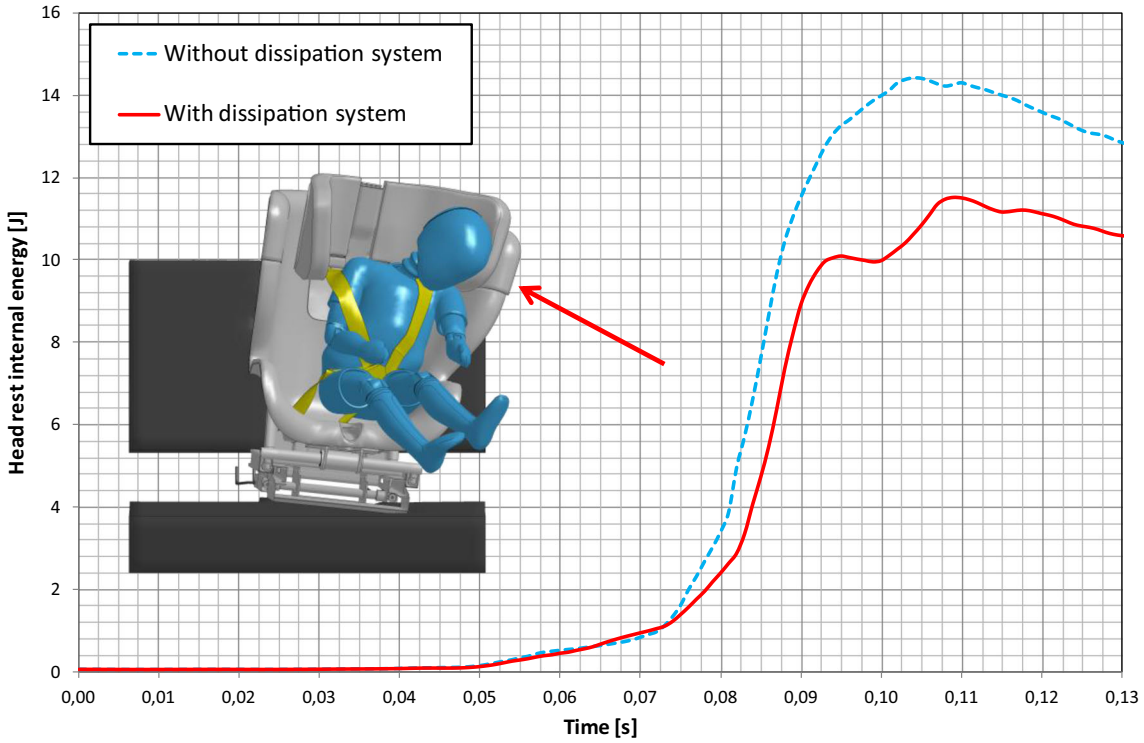

Fig. 10 Internal energy of the CRS headrest in both tests

in test #2: max. 281 J. This is a result of a larger deformation of the CRS parts and especially dissipation elements, the work history of which is represented with a green line. In Fig. 9, a contact force history between ATD's head and the headrest is presented. Due to the presence of dissipation system, the maximum value of force acting on the ATD's head is visibly

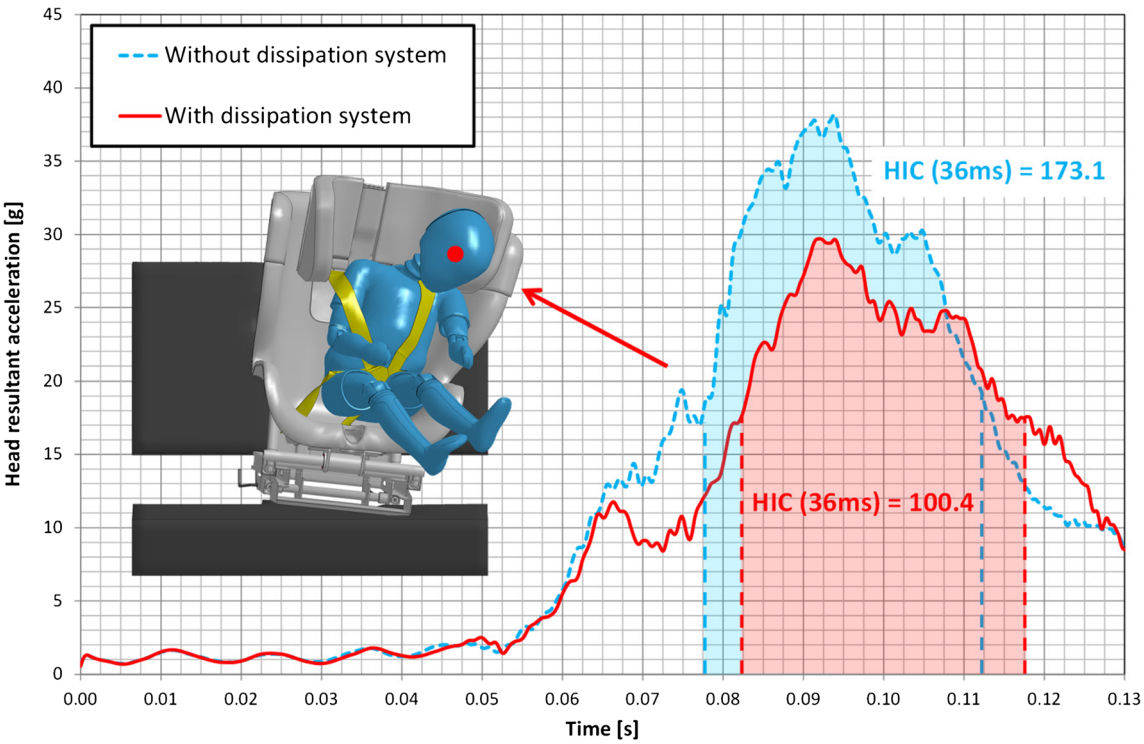

Fig. 11 Resultant acceleration of the ATD's head in both tests

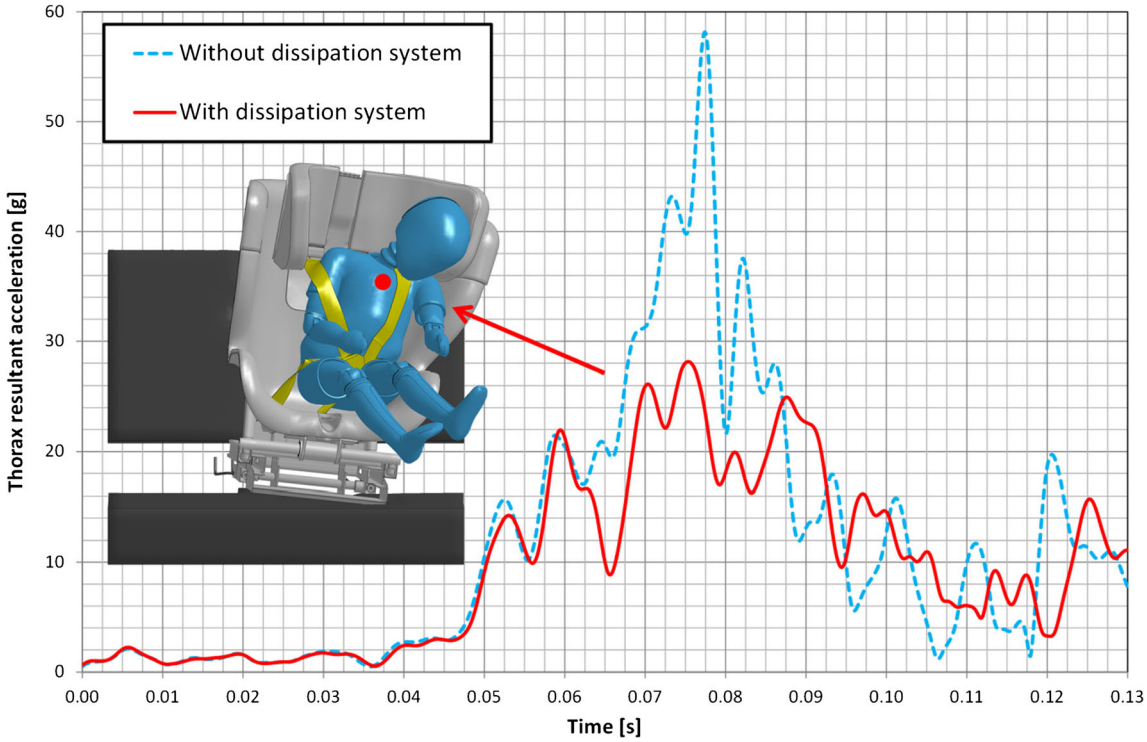

Fig. 12 Resultant acceleration of the ATD's thorax in both tests

smaller (test #2: 632 N), whereas in the basic CRS (test #1), the peak force is 761 N. It is also reflected by the fact that the headrest accumulated smaller amount of energy in test #2: 12 J comparing to 15 J in test #1 (Fig. 10).

Acceleration histories in ATD's head for both cases are shown in Fig. 11. They clearly present that introduction of an energy dissipating mechanism resulted in reduction of the maximum acceleration value by 21% (form 38 to 30 g). One of the most popular injury index: the Head Injury Criteria (HIC), given by (1), was calculated for both acceleration histories based on the following formula:

$$HIC = \max\left[\frac{1}{(t_2-t_1)}\int_{t_1}^{t_2} a(t)dt\right]^{2.5}(t_2-t_1) \quad (1)$$

where $a(t)$ is the acceleration measured in head, t_1 is the beginning of time interval, and t_2 is the end of time interval.

The time interval for the HIC calculation presented below was 36 ms. According to NHCTSA, limiting the HIC limit value for this time interval is 1000 [40]. As predicted, the HIC value obtained for the case with the new energy absorbing system was smaller compared to the case of "basic" CRS. The drop from 173 g in test #1 to 100 g in test #2 means a great improvement of head protection effectiveness by 42% (see Fig. 11).

Acceleration histories measured in the ATD's thorax are shown in Fig. 12. Again, introduction of dissipation system resulted in smaller peak acceleration values (test #2: 28 g, test #1: 58 g). From the obtained results, it can be concluded that in the side impact scenario, the presented system of energy dissipation is very effective. It is worth noticing that simulations were conducted using Q3 ATD series. This series represents the most difficult case to protect a group of children. They are old enough to be transported in front-seated restraint systems; however, on the other hand, all the other biomechanical parameters of the body do not allow for implementation of seatbelts for adults. In Table 4, the maximum values of all discussed quantities are presented for a more thorough analysis of the simulation results.

From the end-user perspective, the introduced mechanism makes CRS more complicated and heavier. On the other hand, improvement of a protection level compensates these drawbacks with a vengeance.

Table 4 Peak values of discussed quantities of two simulated cases

	CRS elements internal energy [J]	Head—CRS headrest contact force [N]	CRS headrest internal energy [J]	Head res. acceleration [g]	Thorax res. acceleration [g]
Test #-1	216	761	15	173	58
Test #-2	281	632	12	100	28

6 Conclusions

Authors present the idea of a new system allowing for better protection of children transported in CRS during a side (lateral) impact. In the first part, the basic concept of the solution is presented. A number of solutions was analyzed in terms of possibilities for implementation in the CRS prototype. It was decided to use a wire bent on a roll due to its simplicity and, at the same time, high efficiency. In this case, the energy is dissipated via plastic deformation of the introduced dissipation element and to a lesser extent via plastic deformation of CRS parts.

The numerical simulations reflecting a side impact procedure described in UN/ECE Regulation 129 are described subsequently. In the FE analyses, the dissipation elements were modeled using springs elements with a nonlinear force-displacement characteristic obtained from experimental tests. Detailed information on the material data and applied initial-boundary conditions are provided. Finally, the results of simulations comparing the classic CRS with a new solution are presented. A comparison of obtained results shows a great potential behind the proposed energy dissipation system. The main assumption of dissipation system operation was confirmed in the internal energy history of the CRS parts. Due to application of the dissipation elements, a larger amount of energy was consumed. The peak acceleration values in the head and in the thorax of ATD seated in the new CRS were smaller than in case of ATD seated in the "basic" CRS. The same applies to the HIC value. What is also important, the presented solution shows that despite many CRS solutions available on the market, there is still a room for improvement of young passengers' safety. It should be also stated that no real-world tests were carried out with the presented CRS prototype. At present, however, the final CRS ready to be introduced on the market with a dissipation system is being verified and tested to obtain homologation. It is worth noticing, that within the subject of the presented paper the authors carried out other investigations regarding the CRSs and safety of children [41].

Acknowledgements This work has been performed with the financial support from the National Centre for Research and Development (agreement: INNOTECH-K1/IN2/59/182901/NCBR/12). Grant no. RPMA.01.02.00-14-5640/16-00 "Innovative CRS with improved safety parameters" granted within the Mazowieckie Voivodeship ROP 7 "Smart Growth" PA 1.2 "Use of research and development activity in economy" and the support of the Interdisciplinary Centre for Mathematical and Computational Modeling (ICM) University of Warsaw under grant no GB65-19. This support is gratefully acknowledged.

References

1. Naumann RB, Dellinger AM, Zaloshnja E, Lawrence BA, Miller TR (2005) Incidence and total lifetime costs of motor vehicle-related fatal and nonfatal injury by road user type, united states. Traffic Inj Prev 11(4):353–360
2. National Highway Traffic Safety Administration (2014) Traffic safety facts, U.S. department of Transportation, DOT HS 812 261
3. Statistics Canada, major causes of death, Government of Canada, http://www.statcan.gc.ca
4. World Health Organization (2009) European status report on read safety. WHO Regional Office for Europe, Copenhagen
5. Arbogast KB (2014) A public health priority for only ten percent of the car occupant population: why focus on children and how are they different biomechanically? In: Proceedings of the International IRCOBI Conference on the Biokinetics of Impact. Berlin, Germany, September 10–12 2014, 1–14. Available at: http://www.ircobi.org/wordpress/downloads/irc14/pdf_files/01.pdf
6. Koppel S, Muir C, Budd L, Devlin A, Oxley J, Charlton J, Newstead S (2013) Parents' attitudes, knowledge and behaviors relating to safe child occupant travel. Accid Anal Prev 51:18–26
7. Skjerven-Martinsen M, Naess PA, Hansen TB, Staff T, Stray-Pedersen A (2013) Observational study of child restraining practice on Norwegian high-speed roads: restraint misuse poses a major threat to child passenger safety. Accid Anal Prev 59:479–486
8. Jermakian JS, Klinich KD, Orton NR, Flannagan CAC, Manary MA, Malik LA, Narayanaswamy P (2014) Factors affecting tether use and correct use in child restraint installations. J Saf Res 51:99–108
9. Arbogast KB, Ghati Y, Menon RA, Tylko S, Tamborra N, Morgan MR (2005) Field investigation of child restraints in side impact crashes. Traffic Inj Prev 6(4):351–360
10. Kapoor T, Altenhof W, Howard A, Rasico J, Zhu F (2008) Methods to mitigate injury to toddlers in near-side impact crashes. Accident Anal Prev 40:180–189
11. Suratno B, Job S, Leavy D, Brown J, Paine M, Magedara N, Kelly P, Griffiths M, Haley J, Case M (2008) The Australian Child Restraint Evaluation Program. In: Faulks IJ, Irwin JD (eds) Proceedings of an international conference held in Parliament House, Macquarie Street, Sydney, New South Wales 2-3 August 2007. Report SPAI 2007–24/1. Safety and Policy Analysis International, Wahroonga, pp 445–477
12. Paine M, Griffiths M, Brown J, Case M, Johnstone O (2003) Protecting children in car crashes: the Australian experience. In: Proceedings from the 18th International Technical Conference on the Enhanced Safety of Vehicles (ESV). Nagoya, Japan, May 19–22, 2003. 1–15. Available at: http://citeseerx.ist.psu.edu/viewdoc/download?doi=10.1.1.915.7651&rep=rep1&type=pdf
13. National Highway Traffic Safety Administration (2014) Notice of Proposed Rulemaking: 49 CFR Part 571 Federal Motor Vehicle Safety Standards; Child Restraint Systems— Side Impact Protection, Docket No. NHTSA–2014–0012, RIN 2127–AK95
14. United Nations and Economic Commission for Europe (2014) Regulation No. 129 of the Economic Commission for Europe of the United Nations (UN/ECE)—uniform provisions concerning the approval of enhanced Child Restraint Systems used on board of motor vehicles (ECRS). Official Journal of the European Union
15. Desariya E, Samayawardhena L, Somasiri A, Pike I (2011) Child occupants and side-impact crashes: commentary. J Emerg Nurs 37(4):391–393

16. Decina L, Lococo K (2005) Child restraint system use and misuse in six states. Accid Anal Prev 37:583–590
17. Eby D, Kostyniuk L (1999) A statewide analysis of child safety seat use and misuse in Michigan. Accid Anal Prev 31:555–566
18. Bohman K, Rosén E, Sunnevang C, Boström O (2009) Rear seat occupant thorax protection in near side impacts. Ann Adv Automot Med 53:3–12
19. Fildes B, Charlton J, Fitzharris M, Langweider K, Hummel T (2003) Injuries to children in child restraints. Int J Crashworthiness 8(3):277–284
20. Autoliv (2009) Car to car, 50% overlap at 64 km/h. Toyota Yaris-08 – Volvo 945–96. Internal report. TO- 09000160. Autoliv Research, Vårgårda
21. Dagens Nyheter DN (2009) Small new car is safer (in swedish). Stockholm, Sweden. https://www.dn.se/ekonomi/motor/stor-bil-sakrare-an-liten/
22. Qi W, Jin XL, Zhang XY (2006) Improvement of energy-absorbing structures of a commercial vehicle for crashworthiness using finite element method. Int J Adv Manuf Technol 30:1001–1009
23. Baranowski P, Damaziak K, Malachowski J, Mazurkiewicz L, Muszyński A (2015) A child seat numerical model validation in the static and dynamic work conditions. Arch Civ Mech Eng 15(2): 361–375
24. Pawlus WP, Karimi HR, Robbersmyr KG (2013) Investigation of vehicle crash modeling techniques: theory and application. Int J Adv Manuf Technol 70(5–8):965–993
25. Jamroziak K, Bocian M, Kulisiewicz M (2013) Energy consumption in mechanical systems using a certain nonlinear degenerate model. J Theor Appl Mech 51(4):827–835
26. Pawlus W, Nielsen JE, Karimi HR, Robbersmyr KG (2011) Application of viscoelastic hybrid models to vehicle crash simulation. Int J Crashworthiness 55:369–378
27. Pawlus W, Karimi HR, Robbersmyr KG (2011) Mathematical modeling of a vehicle crash test based on elasto-plastic unloading scenarios of spring-mass models. Int J Adv Manuf Technol 55(1–4):369–378
28. Munyazikwiye B, Karimi HR, Robbersmyr KG (2017) Optimization of vehicle-to-vehicle frontal crash model based on measured data using genetic algorithm. IEEE Access 5:3131–3138
29. Chen Y, Qiao C, Qiu X, Zhao S, Zhen C, Liu B (2016) A novel self-locked energy absorbing system. J Mech Phys Solids 87:130–149
30. Ma J, Hou D, Chen Y, You Z (2016) Quasi-static axial crushing of thin-walled tubes with a kite-shape rigid origami pattern: numerical simulation. Thin-Wall Struct 100:38–47
31. Costas M, Diaz J, Romera LE, Hernandez S, Tielas A (2013) Static and dynamic axial crushing analysis of car frontal impact hybrid. Int J Impact Eng 62:166–181
32. Hu LL, Yu TX (2010) Dynamic crushing strength of hexagonal honeycombs. Int J Impact Eng 37(5):467–474
33. Stephani G, Andersen O, Quadbeck P, Kieback B (2010) Cellular metals for functional applications—an overview. In: structural crashworthiness and failure, Proceedings of PM2010 world congress – Foams & Porous Materials
34. Wierzbicki T, Thomas P (1993) Grounding damage of ships. In: Jones N. Wierzbicki T, ed. Structural Crashworthiness and Failure. London: CRC Press. Proceedings from the Third International Symposium on Structural Crashworthiness held at the University of Liverpool, England, 14–16 April 2009, pp. 467–508
35. Kee Paik J, Wierzbicki T (1997) A benchmark study on crushing and cutting of plated structures. J Ship Res 41(2):147–160
36. Hallquist JO (2006) LS-dyna theory manual. Livermore publishing house. Livermore
37. Belytschko T, Jerry IL, Tsai CS (1984) Explicit algorithms for the nonlinear dynamics of shells. Comput Methods Appl Mech Eng 42: 225–251
38. Muszynski A (2016) Modeling and testing of the child restraint system in terms of reducing the dynamic loads acting on the child body during an accident. PhD thesis, Warsaw, Poland: Military University of Technology
39. Fu S, Kleessen C, Zhou Z, Koschdlo K, Kant R (2011) Development of advanced finite element models of Q child crash test dummies. In: Proceedings from the 8th European users conference, Strasbourg, France, May 23-24, pp 1–23
40. Eppinger R, Sun E, Kuppa S, Saul R (2000) Development of improved injury criteria for the assessment of advanced automotive restraint systems – II. National Highway and Traffic Safety Administration, Washington. Available at: https://www.nhtsa.gov/sites/nhtsa.dot.gov/files/finalrule_all_0.pdf
41. Baranowski P, Damaziak K, Mazurkiewicz L, Malachowski J, Muszynski A, Vangi D (2017) Analysis of mechanics of side impact test defined in UN/ECE Regulation 129. Traffic Inj Prev 19(3): 256–263. https://doi.org/10.1080/15389588.2017.1378813